# Enhancing the performance of the Primary Surveillance Radar using Multilateration

Nicolae CONSTANTINESCU*,[1], Emil CONSTANTINESCU[2],
Alina-Ioana CHIRA[1]

*Corresponding author
[1]INCAS – National Institute for Aerospace Research "Elie Carafoli",
B-dul Iuliu Maniu 220, Bucharest 061136, Romania,
constantinescu.n@incas.ro*, chira.alina@incas.ro
[2]Department of Aeronautical Systems Engineering and Aeronautical Management,
POLITEHNICA University Bucharest,
Splaiul Independentei 313, 060042, Bucharest, Romania,
cconstantinescu2@upb.ro

DOI: 10.13111/2066-8201.2022.14.4.4

*Received: 26 September 2022/ Accepted: 10 November 2022/ Published: December 2022*


***Abstract:*** *One way to improve the measurements of the PSR (Primary Surveillance Radar) is to utilize the cinematic model of the aircraft (A/C) in a Kalman filter. Another newly developed method would be to implement multilateration using a large number of ground-based ADS-B (Automatic Dependent Surveillance-Broadcast) receivers. Originating in airport surveillance, multilateration grew to become the primary system for ATM (Air Traffic Management) in airspaces without PSR coverage. Given that each of the systems has its own advantages and limitations, we propose an evaluation of an alternative approach that uses data from multiple ADS-B receivers to implement a data fusion algorithm between PSR acquired position and MLAT (Multilateration) estimated position. Among the many ways to implement data fusion, have chosen to analyze two possible solutions: the direct fusion of the two available positions provided by the two systems using a traditional Kalman Filter and a linearization approach for the multilateration solution that does not require position computation. In both cases, these will improve the Kalman filter and lower the position estimation errors. The evaluation takes into consideration the possible sources of inaccuracies and provides sensibility analyses in regards to the number and positioning of ADS-B receivers involved in multilateration. This paper will conclude with a discussion of the computational power required for the two implementations.*

***Key Words:*** *Primary Surveillance Radar (PSR), Aircraft (A/C), Multilateration (MLAT), Automatic Dependent Surveillance-Broadcast (ADS-B), Kalman Filter, Air Traffic Management (ATM)*

## 1. INTRODUCTION

Throughout the history of aviation, surveillance has always been a constant topic of discussion because of its importance and the need to constantly improve to adapt the continuous growth of the aviation sector. The bedrock of this system is the Radar system. These systems have been developed and used in a variety of contexts, from aircraft detection and weather and atmosphere mitigation to defensive applications. In aviation, two types of radars stand out: The Primary Surveillance Radar and the Secondary Surveillance Radar. Both of these systems

have been very useful in the early days of Air Traffic Control and Management (ATC/M) however, as stated by the International Civil Aviation Organization Asia and Pacific Office [1], some limitations such as: lack of conventional surveillance, lack of aircraft data (beyond the A/C modes in the case of Secondary Surveillance Radar (SSR)), non-homogeneous operations and lack of capability to support future aviation developments [1], have made it very clear that future research is needed to combat these issues.

One solution for these problems is Multilateration (MLAT). Multilateration is based on the principle of triangulation. The inquiry sent by the secondary radars will generate a response from the aircraft transponder.

After the signal is retransmitted by the aircraft, instead of returning to one single radar station, it is picked up by multiple stations. Alternatively, the aircraft may broadcast periodic signals without the SSR interrogation.

Using the Time Difference of Arrival (TDOA) between the signal and the moving target, we can accurately track the position of the A/C, by limiting it to a certain area, where the lines of equal time differences will intersect. This will help reduce the positioning error and update the A/C location [2]. To demonstrate this, we compare our results with those from other surveillance assessments.

Thus, the purpose of this paper is to establish the importance of MLAT, describe an accurate representation of how MLAT stations should be placed to give us a good representation of the aircraft, to fuse our measurements with other representations of airspace detection, and to consider how we can improve the existing design.

## 2. HYPERBOLIC NAVIGATION

As mentioned in the introduction, the Multilateration system utilized TDOA between the signals and the target to accurately determine the position of the aircraft. To this end, MLAT stations will receive the signal with delays depending on the distance between the aircraft and station; the time difference between any two stations converted into distance will generate hyperbolas (the locus of equal time difference) which in turn will intersect and create an area where the aircraft is currently located.

This is called Hyperbolic Navigation, and the way we identify A/C is by integrating the formula of a Squared Error for a regression line, which will be discussed further in the following chapters [3] [2].

Unlike other techniques of airspace surveillance, Multilateration does not require modifications of aircraft systems (all aircraft are required to carry a Mode A/C/S transponder).

As mentioned in the introduction, for systems that utilize SSR, MLAT intakes the same return signals from the transponder, and when it comes to Traffic Collision Avoidance System (TCAS), it processes the same signals on 1090MHz [4]. In fact, it also serves as a backup method for the Global Navigation Satellite System (GNSS)-based ADS-B reporting system [4]. For the wide-area surveillance method to be properly integrated several criteria need to be considered.

Firstly, the stations showed need to be positioned far apart to ensure the system accuracy and to cover more airspace.

This increases enhances position estimation, but requires more extensive data links infrastructures between receivers [5].

For the purpose of this example, MLAT stations were located at Craiova International Airport (LRCV), Bucharest Henri Coanda International Airport (LROP), and Sibiu International Airport (LRSB), respectively.

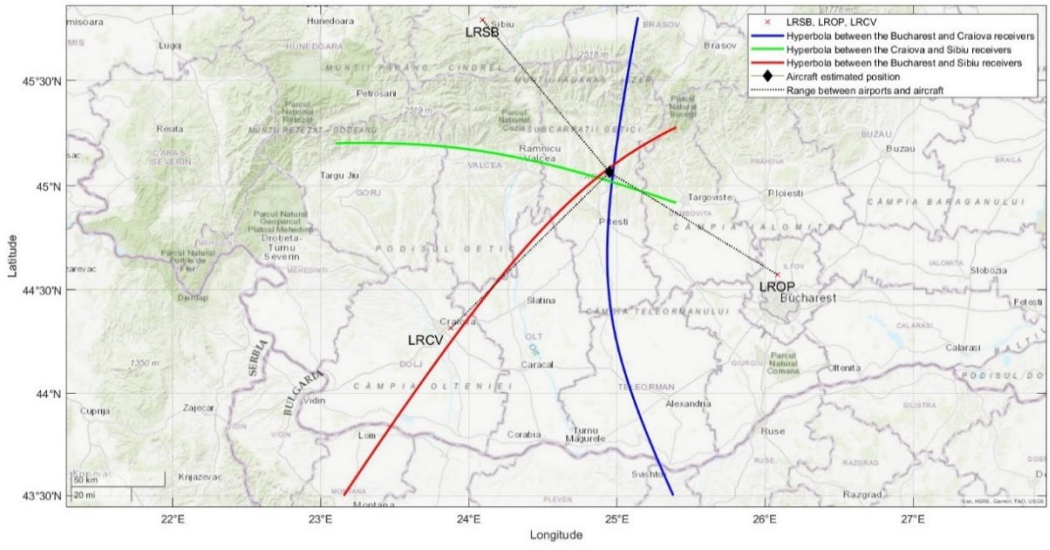


Fig. 1 - Intersection between three TDOA hyperbolas

Because the stations have been positioned correctly, we can see in Fig. 2 what the error surface looks like.

The position is given by the minimum error, which in this case corresponds to a clear Global Minimum.

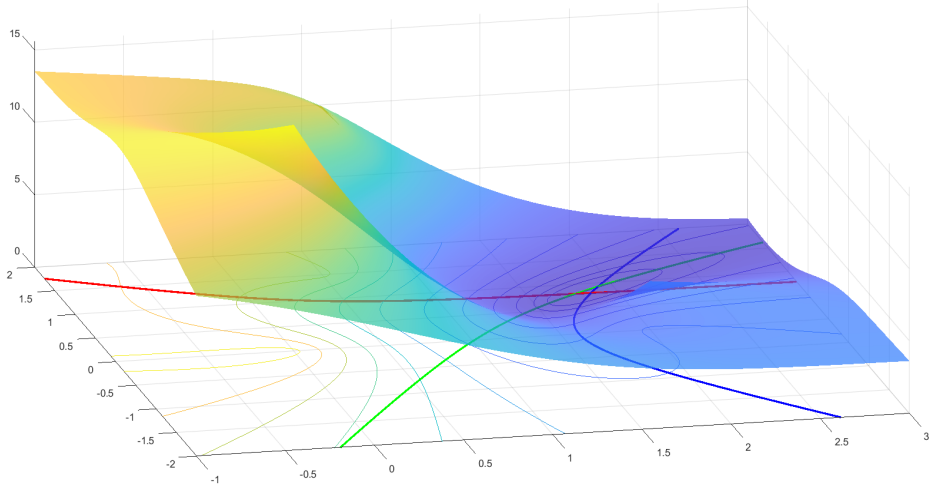

Fig. 2 - Surface representation of MLAT

It is worth mentioning that for this example the altitude of the MLAT system was neglected as it is well documented that this can cause errors in positioning and receiving data from the aircraft.

A 3D representation of the intersection of hyperbolas, seen in Fig. 3, clearly shows how the altitude creates errors in measurement by forming a cone-like volume in which both position and altitude are ambiguous.

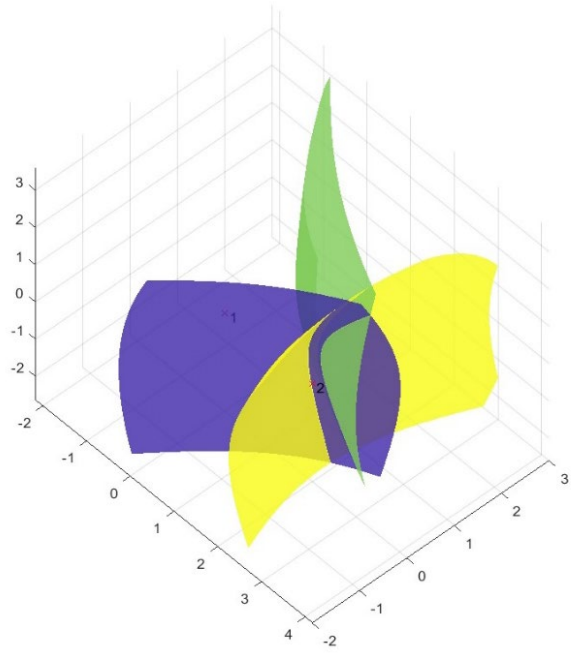


Fig. 3 - Three-dimensional representation of hyperbolic intersection

Another aspect to be considered is the correct position of the receiving stations. As stated, multilateration functions on the principle of triangulation. As such, in order for the surveillance to work, the stations must form a triangular shape to define the time difference between the stations and the target.

If the receivers do not meet this requirement, it will result in an area defined by a high error in location estimation, as shown in Fig. 4, and, compared to Fig. 2, where the aircraft location is given by the global minimum, here the minimum is spread over a wider area without a clear indication of the exact position (Fig. 5).

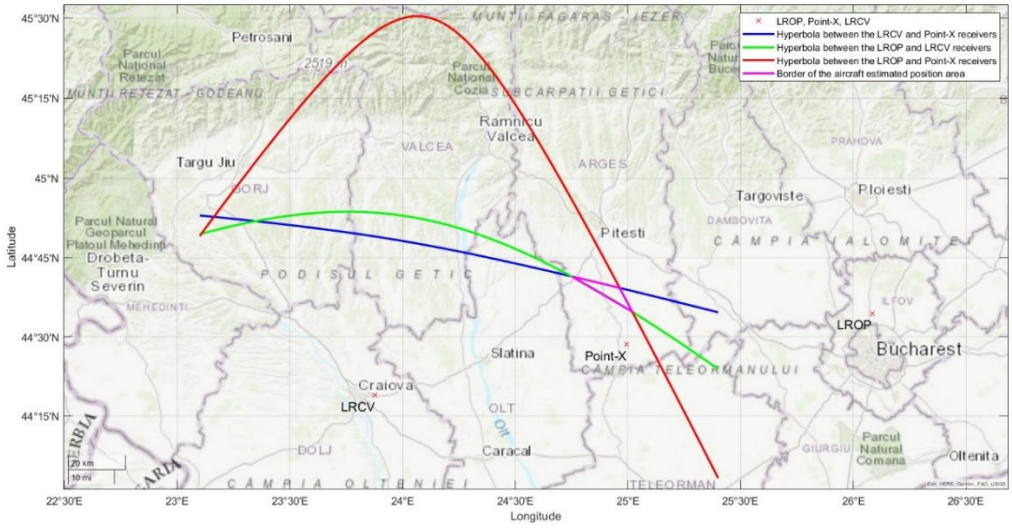


Fig. 4 - Representation of hyperbolic intersection when the MLAT stations are collinear

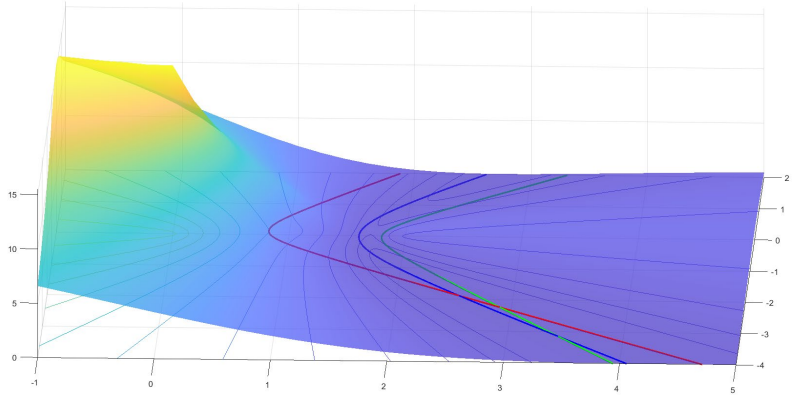

Fig. 5 - Surface representation when the MLAT stations are collinear

To conclude this section, the use of Multilateration seems new in the field of aerospace surveillance, but uses pre-existing methods of radar detection to offer a better assessment of the aircraft's position. The system may have some limitations and errors when implemented improperly and may cause errors related to altitude.

For the next section, we will look at how data fusion can help us get a better picture of how different mathematical models work and how to choose the most accurate solution.

## 3. DATA FUSION

Data fusion, as described in the final paragraph of the last chapter, allows us to integrate different mathematical models into our simulation to better understand the data used, their limitations, and which implementation gives us the best possible results.

We will compare the simulated aircraft's position with the position estimated by radar and that given by multilateration. To show an accurate prediction of the aircraft with respect to the time of the flight, the speed of the A/C, and initial position of the aircraft, we integrated a Kalman Filter. We will utilize the basic form of the simulation to show the behavior of a linear system. Afterward, we used the Extended Kalman Filter to linearize a non-linear system, and finally, to see how the Kalman Filter behaves during non-linearity, we simulated a flight with a turn.

To start, the Kalman Filter is an estimator that blends together consecutive measurements (data inputs) such as speed, position, acceleration, and prediction of the same quantities resulting from the model of the system. It works both for linear and non-linear systems, but, of course, the implementation is simpler in the linear case. The generic equations of the filter are well-known and are as follows:

Given the system in the discreet form:

$$X_k = F \times X_{k-1} + B \times u_k + \omega_k \tag{1}$$

We start by predicting the future output and covariance matrix:

$$P_k = (F \times P_{k-1} \times F^T) + Q \tag{2}$$

$$KG = \frac{P_k \times H^T}{H \times P_k \times H^T + R} \tag{3}$$

$$Y_k - \ new\ infromation\ form\ sensors\ (meseaurements\ at\ time\ k) \tag{4}$$

When the new measurement is available, we correct the prediction:

$$P_{k+1} = (I - KG \times H) \times P_k \times (I - KG \times H) + KG \times R \times KG^T \tag{5}$$

$$X_{k+1} = X_k + KG \times (Y_k - H \times X_k) \tag{6}$$

where

| | |
|---|---|
| $X_k$ | State Matrix |
| $F$ | State Transition Matrix |
| $X_{k-1}$ | Previous State Matrix |
| $B$ | Input Matrix |
| $u_k$ | Control Variable Matrix |
| $\omega_k$ | Predicted State Noise Matrix |
| $P_k$ | Process Covariance Matrix |
| $P_{k-1}$ | Previous Process Covariance Matrix |
| $Q$ | Process Noise Covariance Matrix |
| $KG$ | Kalman Gain |
| $H$ | Observation Matrix |
| $R$ | Measurement Uncertainty |
| $P_{k+1}$ | Next-Step Process Covariance Matrix |
| $I$ | Identity Matrix |
| $X_{k+1}$ | Next Step State Matrix |

The simulations have been done in a two-dimensional format. In the case of a three-dimensional problem, the structure of the matrixes changes accordingly to consider the *z-axis,* but, as discussed above, the problem is not well conditioned geometrically.

For the initial state matrix, we will take the initial position of A/C, but with an initial error (a deviation of 1000 *m* for the position on the *x-axis* and 200 *m* for the position on the *y-axis,* respectively).

We did this to see how the Kalman filter corrects over time. Thus, our matrix will have this form:

$$X_0 = \begin{bmatrix} x_A + 1000 \\ y_A + 200 \\ \dot{x} \\ \dot{y} \end{bmatrix}$$

where $x_A$ is the position of the aircraft on the *x-axis,* $y_A$ is the position of the aircraft on the *y-axis* and $\dot{x}$ and $\dot{y}$ is the velocity of the aircraft on the two axes.

Other matrixes with distinct values worth noting for Kalman implementation are:

$$Q = \begin{bmatrix} 0 & 0 & 0 & 0 \\ 0 & 0.05 & 0 & 0 \\ 0 & 0 & 0 & 0 \\ 0 & 0 & 0 & 0.05 \end{bmatrix}$$

$$H = \begin{bmatrix} 1 & 0 & 0 & 0 \\ 0 & 1 & 0 & 0 \\ 1 & 0 & 0 & 0 \\ 0 & 1 & 0 & 0 \end{bmatrix}$$

$$R = \begin{bmatrix} 200^2 & 0 & 0 & 0 \\ 0 & 200^2 & 0 & 0 \\ 0 & 0 & 100^2 & 0 \\ 0 & 0 & 0 & 100^2 \end{bmatrix}$$

$$F = \begin{bmatrix} 1 & 0 & \Delta t & 0 \\ 0 & 1 & 0 & \Delta t \\ 0 & 0 & 1 & 0 \\ 0 & 0 & 0 & 1 \end{bmatrix}$$

where $\Delta t$ is the timestamp, the moment when the exercise takes place.

The values of Q and R depend on the thrust we put in the system model (Q) and the measurement noise (R). In this case, speed is the derivative of distance, so we do not expect noise to have a large impact, and values of Q are low.

The measurements are unavoidable noisy, so the terms in R have higher values. F and H are obtained directly from the theoretical model.

$$P_k = \begin{bmatrix} 1000 & 0 & 83 & 0 \\ 0 & 310 & 0 & 5 \\ 83 & 0 & 13 & 0 \\ 0 & 5 & 0 & 2 \end{bmatrix}$$

where the numbers in $P_k$ (process covariance matrix) are the steady state values obtained after the first run of the Kalman filter.

To start the surveillance simulation process that will lead us to compare the results using data fusion, we need to determine the position of the A/C. We chose the initial values for latitude and longitude.

These are as follows:

$$lat_A = 44.391969$$

$$lon_A = 27.486180$$

For ease of implementation the coordinates must be Cartesian transformed and this, in turn, requires choosing an arbitrary origin.

Let that be the MLAT station at LROP, which will result in the following conversion formulas:

$$x_A = \frac{(lon_A - lon_{LROP})}{360 \times 2 \times \pi \times R_p \times \cos(lat_{LROP})} \quad (7)$$

$$y_A = \frac{(lat_A - lat_{LROP})}{360 \times 2 \times \pi \times R_p} \quad (8)$$

where $R_p$ is the radius of the Earth (6357 $km$) and $lon_{LROP}$ and $lat_{LROP}$ are latitude and longitude of the hypothetical MLAT station placed at Henri Coanda International Airport (LROP) in Bucharest, with their respective values being:

$$lat_{LROP} = 44.573190$$

$$lon_{LROP} = 26.091557$$

Let first consider a rectilinear, uniform movement of the target. In order to update the position of the A/C, we will be using the following update formulas:

$$lat_A = lat_A + \cos(psi) \times \frac{\frac{TAS \times \Delta t}{3600}}{60} \tag{9}$$

$$lon_A = lon_A + \sin(psi) \times \frac{\frac{TAS \times \Delta \mathrm{t}}{3600}}{60 \times \cos(lat_A)} \tag{10}$$

where $TAS$ is the true airspeed in knots and $psi$ is the track angle ($120^o$).

These will give us the actual position of the aircraft, which will be compared to other methods of surveillance. To determine the velocity on the axis, we will use the following formulas:

$$\dot{x} = TAS[kt] \times \sin(psi) \times 0.514 \left[\frac{m/s}{kt}\right] \tag{11}$$

$$\dot{y} = TAS[kt] \times \cos(psi) \times 0.514 \left[\frac{m/s}{kt}\right] \tag{12}$$

Now, for the next step in the data filtering process, we need to determine the points in which the radar hits our aircraft. In order to do so, we will first have to determine the position of the ground-based radars.

For this, we will use the same formulas as those used to determine the location of the airport, but adapting them for the coordinates of the radars.

$$x_A = \frac{(lon_R - lon_{LROP})}{360 \times 2 \times \pi \times R_p \times \cos(lat_{LROP})} \tag{13}$$

$$y_A = \frac{(lat_R - lat_{LROP})}{360 \times 2 \times \pi \times R_p} \tag{14}$$

where $lon_R$ is the longitude of the radars and $lat_R$ are the latitude of the radars.
In our case, the stations will be located in Turnu Măgurele, București, Pitești and Bacău. The main characteristics measured by the radars are the range ($\rho$) and bearing ($\theta$), which will be calculated using basic radar equations:

$$\rho = \sqrt{\left(\frac{(lat_A - lat_{LROP})}{360 \times 2 \times \pi \times R_p}\right)^2 + \left(\frac{(lon_A - lon_{LROP})}{360 \times 2 \times \pi \times R_p \times \cos(lat_{LROP})}\right)^2} \tag{15}$$

$$\theta = atan2((lon_A - lon_{LROP}) \times \cos(lat_{LROP}), (lat_A - lat_{LROP})) \tag{16}$$

To update the next measurements, we need to account the accuracy in bearing measurements, the systemic propagation of range for the standard atmosphere, and the size of the aircraft to account for the position where the radar wave hits the A/C.

$$\rho = \rho + ((0.05 \times 10^{-6} + 0.12^{-6}) \times c + 34) \times \mu \tag{17}$$

$$\theta = \theta + 0.16 \tag{18}$$

where $c$ is the speed of light and $\mu$ is the noise.
According to [6] accuracy in bearing is MSSR-2000 <±0.049°.

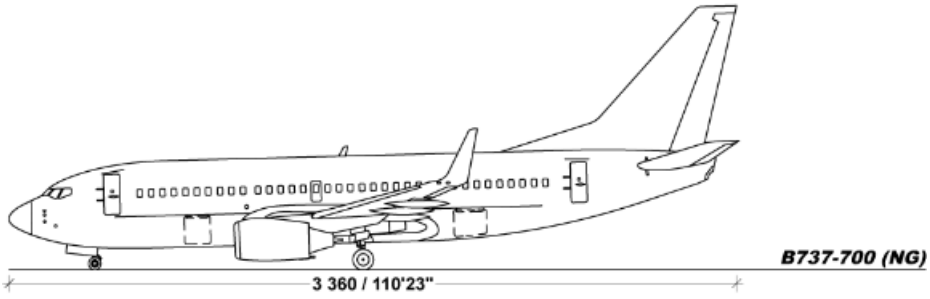


Fig. 6 - Specification -Boeing 737-700 [7]

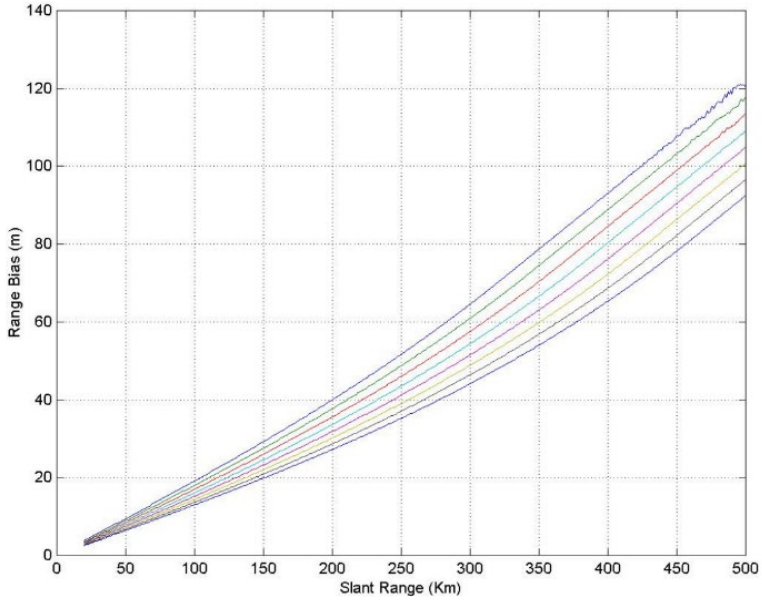


Fig. 7 - Systematic error due to propagation for the standard atmosphere [8]

To simulate MLAT, we also need to determine the time it takes for the signal to propagate:

$$tR = \frac{d}{c} + tA \tag{19}$$

where $tR$ is the reception time and $tA$ is the unknown transmission return time from the aircraft. This value will also need to be updated with respect to the previous values.

$$tR = tR_0 - t_{min} + \mu \times (0.05 \times 10^{-6} + 0.12 \times 10^{-6}) \tag{20}$$

We now utilize the formula for squared error for the regression. This will show us how accurate the MLAT detections are compared to the actual position of the aircraft by squaring the errors.

$$\begin{aligned} SE_{line} = (y_1 - (m \times x_1 + b)^2 + (y_2 - (m \times x_2 + b)^2 + \cdots \\ + (y_1 - (m \times x_1 + b)^2 + (y_n - (m \times x_n + b)^2 \end{aligned} \tag{21}$$

where $m$ is the slope, $b$ is the y-axis intercept and $x_{1\ldots n}$, $y_{1\ldots n}$ are the coordinates of the MLAT detections.

This will yield the coordinates for multilateration, $x_{mlat}$ and $y_{mlat}$. Regarding the errors mentioned earlier, the formula will be as follows:

$$err_{mlat} = \sqrt{(x_A - x_{mlat})^2 + (y_A - y_{mlat})^2} \tag{22}$$

For the detections of the radar, we will take the range between the radar and target and bearing between the antenna direction and the true north.

$$x_{rad} = \rho \times \sin(\theta) \tag{23}$$

$$y_{rad} = \rho \times \cos(\theta) \tag{24}$$

where $x_{rad}$, $y_{rad}$ are the coordinates of the where the radar detected the aircraft.

We also need to take into consideration the minimum error between the position of the RADAR detection and the actual position of the aircraft:

$$err_{radar} = \sqrt{(x_A - x_{rad})^2 + (y_A - y_{rad})^2} \tag{25}$$

We can finally implement the Kalman Filter based on the MLAT and radar detections. However, the state and measurement state matrices have to be updated:

$$X_k = \begin{bmatrix} x_{rad} \\ y_{rad} \\ \dot{x} \\ \dot{y} \end{bmatrix} \tag{26}$$

$$Y_k = \begin{bmatrix} x_{rad} \\ y_{rad} \\ x_{mlat} \\ y_{mlat} \end{bmatrix} \tag{27}$$

All these measurements can be added together to compare the different methods of A/C detection (Fig. 8) where we can clearly see that the Kalman Filter fused with the MLAT surveillance is the best possible solution.

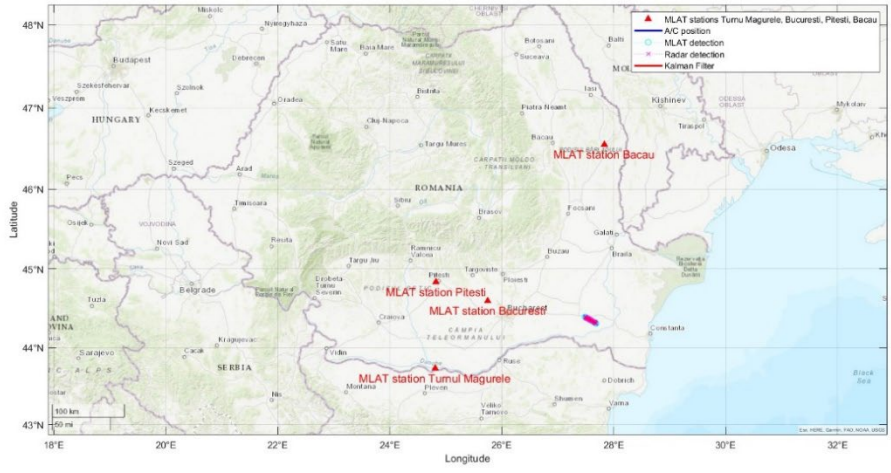

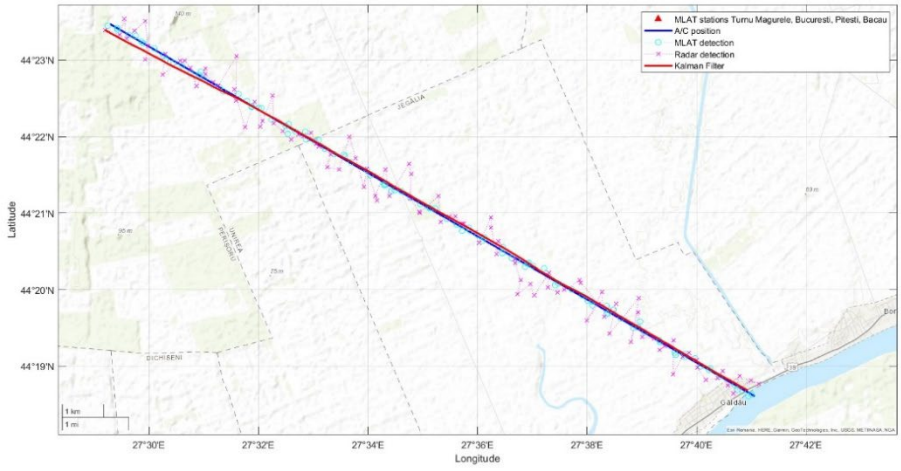


Fig. 8 - Data fusion utilizing the Kalman Filter

The next step of the simulation will be the integration of the Extended Kalman Filter. The Extended Kalman Filter (EFK) is similar in practice to the Kalman Filter, using the same base equations as the original filter, however it differs by trying to approximate the State matrix as a Gaussian process and also by using the 2nd order derivative for system approximation of the non-linear dynamics.

It does so, by changing the Cartesian coordinates into polar ones and by applying the Jacobian Observation Matrix with respect to the time and distance between the four MLAT stations.

$$\rho = \sqrt{x^2 + y^2} \tag{28}$$

$$\theta = \arctan\left(\frac{y}{x}\right) \tag{29}$$

$$d_{ij} = \frac{\sqrt{(x - x_i)^2 + (y - y_i)^2}}{c} - \frac{\sqrt{\left(x - x_j\right)^2 + \left(y - y_j\right)^2}}{c} \tag{30}$$

$$H_J = \begin{bmatrix} \frac{\partial \rho}{\partial x} & \frac{\partial \rho}{\partial y} & \frac{\partial \rho}{\partial \dot{x}} & \frac{\partial \rho}{\partial \dot{y}} \\ \frac{\partial \theta}{\partial x} & \frac{\partial \theta}{\partial y} & \frac{\partial \theta}{\partial \dot{x}} & \frac{\partial \theta}{\partial \dot{y}} \\ \frac{\partial d_{12}}{\partial x} & \frac{\partial d_{12}}{\partial y} & \frac{\partial d_{12}}{\partial \dot{x}} & \frac{\partial d_{12}}{\partial \dot{y}} \\ \frac{\partial d_{23}}{\partial x} & \frac{\partial d_{23}}{\partial y} & \frac{\partial d_{23}}{\partial \dot{x}} & \frac{\partial d_{23}}{\partial \dot{y}} \\ \frac{\partial d_{34}}{\partial x} & \frac{\partial d_{34}}{\partial y} & \frac{\partial d_{34}}{\partial \dot{x}} & \frac{\partial d_{34}}{\partial \dot{y}} \\ \frac{\partial d_{13}}{\partial x} & \frac{\partial d_{13}}{\partial y} & \frac{\partial d_{13}}{\partial \dot{x}} & \frac{\partial d_{13}}{\partial \dot{y}} \end{bmatrix} \tag{31}$$

$$Y_k = \begin{bmatrix} \rho \\ \theta \\ d_{12} \\ d_{23} \\ d_{34} \\ d_{13} \end{bmatrix} = \begin{bmatrix} \rho \\ \theta \\ t_{R_1} - t_{R_2} \\ t_{R_2} - t_{R_3} \\ t_{R_3} - t_{R_4} \\ t_{R_1} - t_{R_3} \end{bmatrix} \tag{32}$$

where $\rho$ is the radial distance, $\theta$ is the measured angle, $H_J$ is the Jacobian Observation Matrix, $d_{ij}$ is the generic form for the distances $d_{12}$ ,the distance between Târgul Mureș and București stations, $d_{23}$, the distance between București and Pitești stations, $d_{34}$ ,the distance between Pitești and Bacău and $d_{13}$ which is the distance between Turnu Măgurele and Pitești.

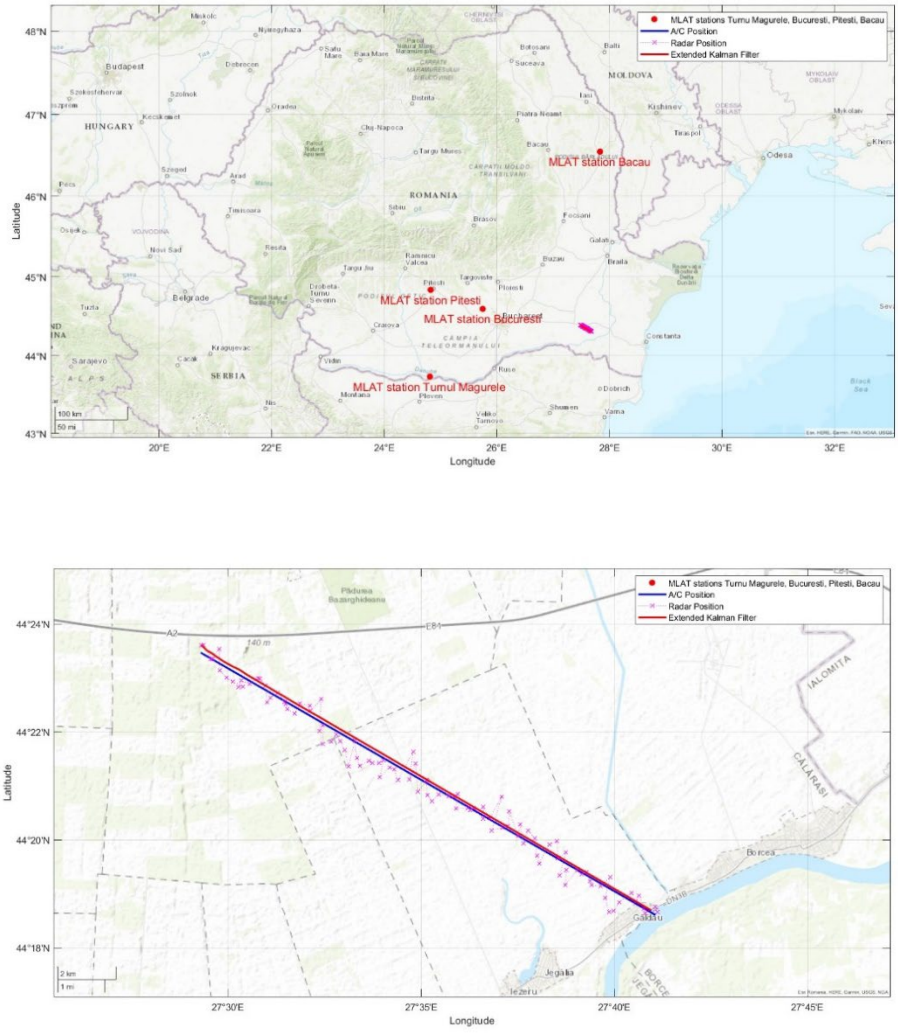


Fig. 9 - Data fusion utilizing the Extended Kalman Filter

Now we come to a variation of the Extended Kalman Filter where we deal with a sudden turn. In this case, the equation for the next state measurement matrix has to be adapted for the predicted measurement of the state.

This is because we are no longer dealing with a linear system of coordinates which can be easily predicted and so we have to account for the difference between the initial measurement of state and the predicted one. And so, the new equation for the state matrix will be as follows:

$$X_{k+1} = X_k + KG \times (Y_k - Y_{pr}) \tag{33}$$

where $Y_{pr}$ is the predicted measurement of the state.
The following example will also contain a deviation of the initial position of the Kalman to show how the filter stabilizes overtime.

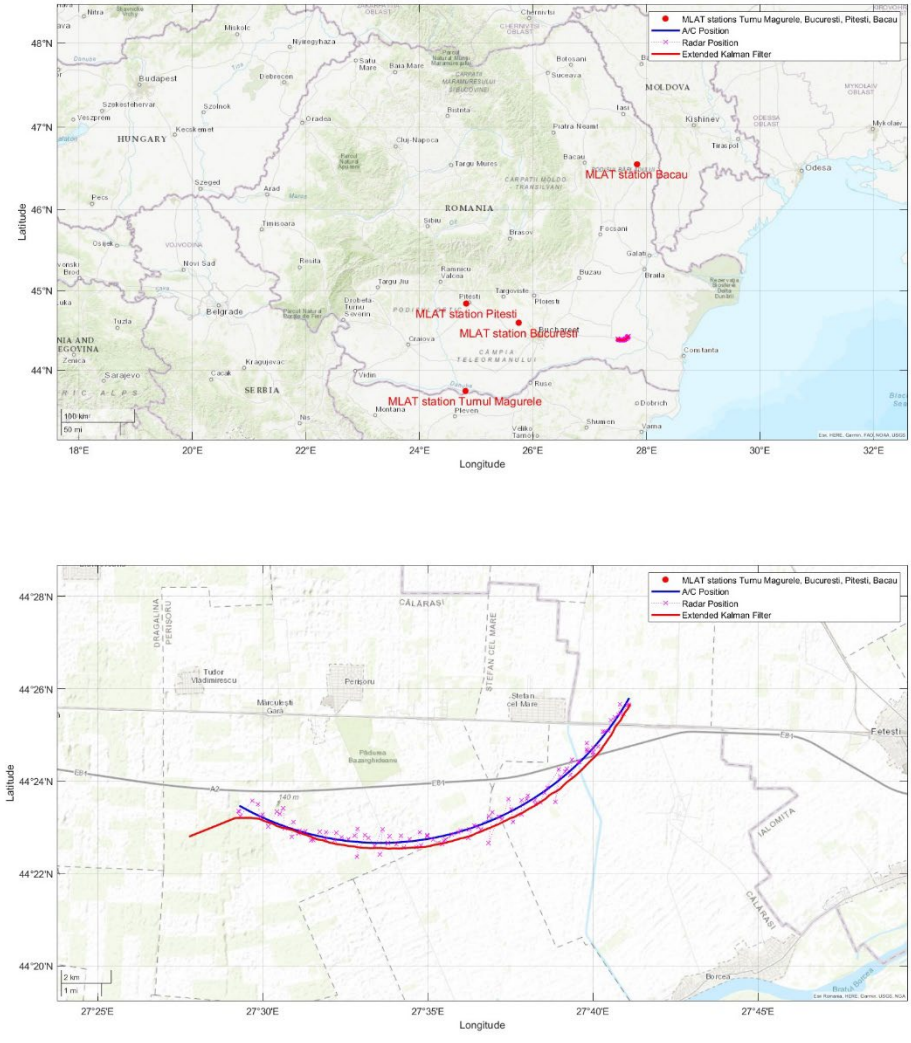


Fig. 10 - Data fusion utilizing the Extended Kalman Filter for a turn

## 4. CONCLUSIONS

To sum up, Multilateration is a complex solution that requires a good understanding of previous methods of radar detection and how they work. The position of MLAT stations is necessary for the correct detection of a target.

As such, if the stations were collinear, it would create a large margin of error A/C positioning area. Furthermore, given a traffic pattern for the location of MLAT stations, they may be subject to an optimization problem.

The integration of the two Kalman filters into MLAT provides us with a better understanding of how the A/C position and its respective velocity changes over time. The implementation of both the radar detection and MLAT position into the Kalman Filter allows a higher degree of accuracy.

From the previous simulations, we can see how the Extended Kalman Filter is much more reliable than the Linear Kalman Filter, as it provides us with a better view of the resulting values in the real-world; it requires less computational power and the timing is more predictable.

## 5. FUTURE WORK

The final part of this article focuses on ways in which simulation solutions can be improved in future research. As stated at the beginning, an error that occurs in Multilateration (MLAT) is the altitude at which the stations are positioned. In the future, we would like to implement those measurements to provide an accurate depiction of detection.

As mentioned in the conclusion**,** the method we found the most suitable for our case study was combining MLAT with a Kalman Filter utilizing A/C position. In the future, we will consider all the RADAR measurements as they have proven to be very unreliable.

Finally, we looked at collision avoidance in automated machine tools. Although, there is no existing method suitable to fix this problem, the integration of the Doppler Shift into an Extended Kalman Filter for non-linear estimation seems to be a good solution for single-target tracking over short distances. For this approach, the method of Maximum Likelihood is used for initialization [9].

## ACKNOWLEDGEMENT

This article is an extension of the paper presented at *The International Conference of Aerospace Sciences, "**AEROSPATIAL 2022**"*, 13 – 14 October 2022, Bucharest, Romania, Hybrid Conference, Section 7 – ATS and full Automation ATM.

## REFERENCES

[1] * * * INTERNATIONAL CIVIL AVIATION ORGANIZATION ASIA AND PACIFIC OFFICE, *Multilateration (MLAT) Concept of use*, September 2007.

[2] A. Mathias, M. Leonardi and G. Galati, An Efficient Multilateration Algorithm, in *Proceedings of ESAV'08* - September 3 - 5 - Capri, Italy, 2008.

[3] H. B. Lee, *Accuracy Limitations of Hyperbolic Multilateration Systems*, Technical Note 1973-11, Lexington, Massachusetts, 1973.

[4] N. Xu, R. Cassell, C. Evers, S. Hauswald, W. Langhans, *Performance assessment of Multilateration Systems – a solution to nextgen surveillance*, Published 11 May 2010, Computer Science, 2010 Integrated Communications, Navigation, and Surveillance Conference Proceedings, DOI:10.1109/ICNSURV.2010.5503290.

[5] Sherman C. Lo, Per Enge, Capacity Study of Multilateration (MLAT) based Navigation for Alternative Position Navigation and Timing (APNT) Services for Aviation, *Navigation Journal*, vol. **59**, no. 4, February 2012.
[6] C. Wolff, *radartutorial.eu*, [Online], Available: https://www.radartutorial.eu/01.basics/Radars%20Accuracy.en.html.
[7] J. Scavini, *Wikimedia commons*, 20 October 2011, [Online], Available: https://commons.wikimedia.org/wiki/File:Boeing_737_family_v1.0.png.
[8] G. de Miguel Vela, J. Besada Portas, J. García Herrero, Correction of propagation errors in Wide Area Multilateration systems, in *Proceedings of the 6th European Radar Conference*, Rome, 2009.
[9] T. J. Mittermaier, U. Siart, T. F. Eibert, and S. Bonerz, Extended Kalman Doppler tracking and model determination for, *Adv. Radio Sci.*, **14**, 39–46, 28 September 2016.